NTNU

Norwegian University of
Science and Technology

Wind Effects on a Sports Arena

Sven-Håkon Wold Sundt

Master of Science in Mechanical Engineering
Submission date: June 2016
Supervisor: Lars Sætran, EPT

Norwegian University of Science and Technology
Department of Energy and Process Engineering

NTNU
Norwegian University
of Science and Technology

Department of Energy
and Process Engineering

EPT-M-2016-134

MASTER THESIS

for

Student
Sven-Håkon Wold Sundt

Spring 2016

Wind effects on a sports arena

Vind-effekter på et idrettsanlegg

The presence of buildings significantly changes the local wind climate. The factors that make up the outer atmosphere of the buildings are: force and direction of wind, its velocity, air pollution, rain-drops and debris lifted and transported with the wind, and sunshine. Each of these factors depends on the shape, size and orientation of buildings to the direction of wind flow and their interaction with surrounding buildings or other landscape elements in the environment [Blocken and Carmeliet 2004].

Increased wind velocity around building may lead to uncomfortable or even dangerous conditions for pedestrians, while decreased wind speeds lead to insufficient removal and accumulation of pollutants of various origins, such as dust, gaseous pollutants, odors, garbage, acoustic effects. Discomfort due to wind velocity at pedestrian level is one of the problems that are considered most important. In the framework of the European COST Action C14, the first Working Group has gathered various wind comfort criteria with the purpose of discussing the present state-of-the-art, identifying differences, and initiating a common criterion or code of good practice [Koss 2006].

For the present work we propose to build a model of a building (a sports arena in the design stage), with surrounding buildings and terrain, and to study the load effects from wind and to identify effects of the wind on the pedestrian level

References:
Blocken B., Carmeliet J., 2004. Pedestrian wind environment around buildings: Literature review and practical examples. J. Therm. Envel. Build. Sci. 28(2).
Koss H.H., 2006. On differences and similarities of applied wind comfort criteria. J. Wind Eng. Ind. Aerodyn., 94.

Within 14 days of receiving the written text on the master thesis, the candidate shall submit a research plan for his project to the department.

When the thesis is evaluated, emphasis is put on processing of the results, and that they are presented in tabular and/or graphic form in a clear manner, and that they are analyzed carefully.

The thesis should be formulated as a research report with summary both in English and Norwegian, conclusion, literature references, table of contents etc. During the preparation of the text, the candidate should make an effort to produce a well-structured and easily readable report. In order to ease the evaluation of the thesis, it is important that the cross-references are correct. In the making of the report, strong emphasis should be placed on both a thorough discussion of the results and an orderly presentation.

The candidate is requested to initiate and keep close contact with his/her academic supervisor(s) throughout the working period. The candidate must follow the rules and regulations of NTNU as well as passive directions given by the Department of Energy and Process Engineering.

Risk assessment of the candidate's work shall be carried out according to the department's procedures. The risk assessment must be documented and included as part of the final report. Events related to the candidate's work adversely affecting the health, safety or security, must be documented and included as part of the final report. If the documentation on risk assessment represents a large number of pages, the full version is to be submitted electronically to the supervisor and an excerpt is included in the report.

Pursuant to "Regulations concerning the supplementary provisions to the technology study program/Master of Science" at NTNU §20, the Department reserves the permission to utilize all the results and data for teaching and research purposes as well as in future publications.

The final report is to be submitted digitally in DAIM. An executive summary of the thesis including title, student's name, supervisor's name, year, department name, and NTNU's logo and name, shall be submitted to the department as a separate pdf file. Based on an agreement with the supervisor, the final report and other material and documents may be given to the supervisor in digital format.

X ☐ Work to be done in lab (Water power lab, Fluids engineering lab, Thermal engineering lab)
☐ Field work

Department of Energy and Process Engineering, 18. January 2016

Olav Bolland
Department Head

Lars Sætran
Academic Supervisor

Sammendrag

En analyse av vindeffektene på en skalamodell av Maier arena har blitt gjort. Tre forskjellige typer eksperimenter ble utført ved åpent landskap og med bygninger rundt. Eksperimentene ble utført for sør, sørvest og vest vindretning. For åpent landskap kan alle vindretninger antas testet på grunn av symmetrisk modell. Et Reynolds nummer uavhengig atmosfærisk grensesjikt ble benyttet ved alle testene.

Reynolds nummer uavhengige trykk koeffisienter for arenaen ble funnet. Maksimalt positivt veggtrykk var 0.15, maksimalt negativt veggtrykk koeffisient var 0.28, maksimalt negativt taktrykk var 0.33.

To typer strømningsvisualiseringseksperimenter ble utført. Retningsvisualisering ved å bruke knappenåler til å feste tråder. Retninger ble påvist og områder hvor resirkulerende strømning oppstår ble påvist. De ble funnet under taket, tråden pekte mot vindretningen.

Det andre visualiseringseksperimentet ble gjort med å jevnt fordele et pulver over modellen. Deretter ble bilder tatt av pulverfordelingen, ved to forskjellige vindhastigheter. Der pulveret ble liggende igjen kunne det påvises separasjon. Der pulveret ble fjernet er det tydelig at vinden har dannet grensesjikt på ny med modellen. Dette forteller om hvor på isbanen vinden vil påvirke.

Kort og langtids vindroser ble hentet fra meteorologisk institutts nettside. De vanligste vindretningene var sør, sørvest. Vinden i området overgår sjelden vindbehag kriterier. Takskader oppstår oftest på grunn av sammenbrudd ved kanten på taket. I følge forskning er vindlastene på taket avhengig av høyden, mens vegglastene mer eller mindre er uberørt.

Wind effects on a sports arena

Sven-Håkon Wold Sundt, *NTNU*

***Abstract*—Wind effects on a scale model of the Maier sports arena have been investigated with three different experiment types. The experiments were performed with "open land" and "nearby structures", with south, southwest and west wind direction. Due to symmetry, the open land experiments are valid for north, northwest, northeast, east and southeast. A Reynolds number independent atmospheric velocity profile simulation was generated in the wind tunnel. Reynolds number independent mean pressure coefficient distribution was determined for the arena. The results obtained for the windward wall indicate a maximum positive pressure coefficient of 0.16 and maximum negative pressure coefficient of 0.28. At the roof, a maximum negative pressure coefficient of 0.33 was found. Flow visualization was performed to identify flow behavior. Recirculation was observed on the ground, under the roof. Separation at the leading edges of the roof was demonstrated due to the lack of powder removal. Worst case for powder accumulation was found to be from southwest (and due to symmetry, southeast, northwest and northeast). Reattachment occurred downstream, leading to removal of powder, thus visualizing where high wind speeds will be occurring for the tested wind directions. Meteorological data indicated most frequently wind from south and southwest. The wind speed of this area was found to rarely exceed wind comfort criteria. The literature review confirms and sheds further light onto the results. Roof failure is the most common cause for structural damages, and is mainly caused by failures at the windward edges during peak loads.**

***Index Terms*— Small scale wind tunnel testing, pressure distribution, flow visualization, site roughness evaluation, meteorological data**

I. INTRODUCTION

WIND produces several effects on buildings and the environment. When designing and dimensioning buildings, it is important to investigate the maximum loads likely to affect the structure. Hence, the forces produced by the wind are of interest. Wind also affects the pedestrian comfort around and inside the structure. Unfortunate design may produce bottlenecks where wind speeds drastically increase and create discomfort or dangerous situations. In addition, snow drifting and accumulation can affect the structure in a significant manner.

This paper will determine the wind effects on the Maier arena, which is to be built in Tønsberg. A small scale model of the sports arena has been built and wind tunnel tested. The nearby environment significantly affects the local wind climate. This includes roughness of the terrain, presence of nearby buildings and changes in elevation. An atmospheric boundary layer will be simulated in the wind tunnel to achieve realistic results.

The finished scale model was tested in wind tunnel experiments. The pressure coefficients at certain points on the arena was determined by using static pressure tubes. Several wind directions were tested, evaluated and compared. In addition, flow visualization was done to determine the wind behavior inside, outside and on the arena. Finally, the results were compared to what has been found in previous research.

II. THEORY

A. Atmospheric velocity profile

Wind speed in the atmosphere varies with height. At the ground the velocity is zero due to the no-slip condition [1]. Obstacles in the terrain slow down the wind and introduces randomness in the vertical and horizontal wind direction [2]. It is not practical to measure the atmospheric boundary layer height and profile; therefore, an extrapolation method is used instead. The power law equation is one such method [3]

.

$$U(z) = U(H)\left(\frac{z}{H}\right)^{\alpha} \quad (1)$$

Equation (1) is based on U(H), a reference wind speed measurement at reference height H. It is common to use 10 minutes averaging measurement taken at a reference height of 10 m [3]. The exponent α, is dependent on the roughness. Higher roughness indicates a higher value for α, which leads to lowered wind speeds at ground. The opposite is also true. Lower roughness, lower value for α, higher wind speeds at ground.

B. Bernoulli's equation

"Bernoulli's equation states that the sum of the flow, kinetic and potential energies of a fluid particle along a streamline is constant. Therefore, the kinetic and potential energies of the fluid can be converted to flow energy (and vice versa) during flow, causing the pressure to change [4]". This means an increase of fluid speed occurs simultaneously with a decrease in pressure or decrease in the fluid potential energy (and vice versa). Some assumptions must be made.

1) *The flow must be steady.*
2) *The flow must be incompressible*
3) *Friction by viscous forces must be negligible*

The wind tunnel does not provide perfectly steady flow, but can be assumed to. Wind speed is low, so the air can be assumed to behave incompressible. Viscous forces can be assumed to be negligible as well.

$$p + \frac{1}{2}\rho U^2 = p_0 \quad (2)$$

Equation 2 is the Bernoulli equation multiplied by density [4], and simplified by assuming that the change in height z along the streamline is negligible compared to the other terms. The sum of static pressure plus dynamic pressure is equal to the total pressure. A pitot tube enables one to measure the difference between the total pressure and the static pressure, i.e. the dynamic pressure.

$$U = \left(2\frac{p_0 - p}{\rho}\right)^{\frac{1}{2}} \quad (3)$$

By rearranging equation 2, equation 3 is obtained. Wind speed can thus be determined at a point in the flow.

C. Flow separation and reattachment

When an object is exposed to a flow, a boundary layer will form at the object. A change in geometry changes the boundary layer. At the wall of the arena, the wind will slow down and pressure will increase, as expected from equation 2. At the roof, wind speed will increase and pressure will reduce.

At the roof, flow detachment, i.e. separation may occur. Flow separation occurs when the fluid reaches high speeds and changes in geometry, in addition, velocities are lowered at the separated flow regions [4].

Separation will also occur when the wind leaves the roof and flows towards the ground, leading to recirculation at the area below and suction on the walls. For roofs of certain length, the wind will reattach onto the roof. The wind may also reattach to the ground of the arena.

D. Pressure coefficient

The pressure coefficient is a dimensionless number obtained by dividing the difference between pressure at a point and freestream, by the dynamic pressure [5]. Shown in equation 4.

$$C_p = \frac{p - p_\infty}{\frac{1}{2}\rho_\infty U_\infty^2} \quad (4)$$

If the pressure coefficient is determined to be Reynolds number independent, the results can be scaled. This means the results can be evaluated for a wide range of wind speeds.

III. Modelling

A. *Small scale arena*

The accuracy of the wind tunnel testing is dependent on the accuracy of the constructed model. A scale of 1:150 was chosen for easing the construction and handling of the model. See Fig. 1 for dimensions. The model was hand built. Some inaccuracies in the model occurred. The built model has a taller roof than planned. The final scale in height was 1:132. The roof has an incline of 5.8°.

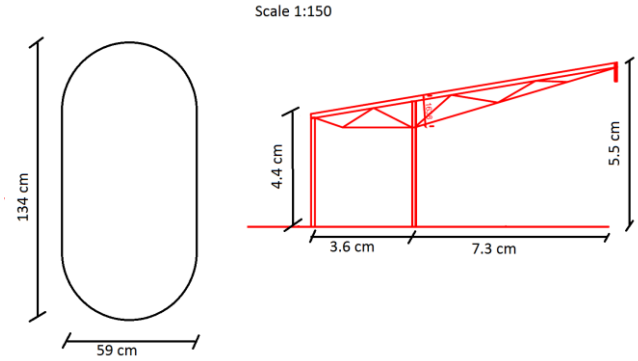

Figure 1: Main dimensions

Figure 2: Finished model of the Maier Arena

In order to test for wind pressure, the model is equipped with static pressure tubes at four sections. North (C), South (A), East (D) and West (B). There are 5 pressure taps at each section. Two on the wall and roof, and one under the roof. This enables the external pressure distribution on the wall and roof to be determined. In addition, the pressure under the roof is interesting to determine the wind effects experienced by the spectators under the roof. Fig. 3 shows the pressure tap sections, and the pressure tap location in each section.

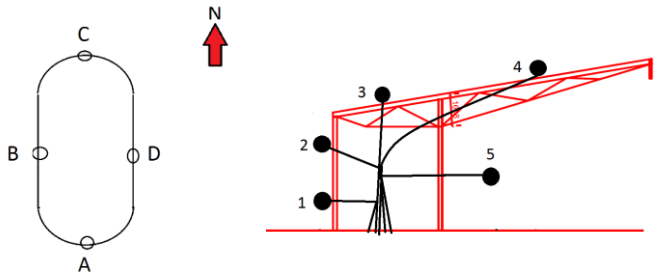

Figure 3: Pressure tap sections and location

B. *Nearby structures*

The nearby structures, see Fig. 4 below, were modelled by cutting blocks at a height of 4.8 cm and shaping and positioning them into the form and position shown below. A simplification with flat roof was done because of time limitations. Further refinement of the structures could be done to achieve more accurate results. Nevertheless, the inclusion of these bricks produces some additional information regarding the wind effects over the arena when experiencing cover.

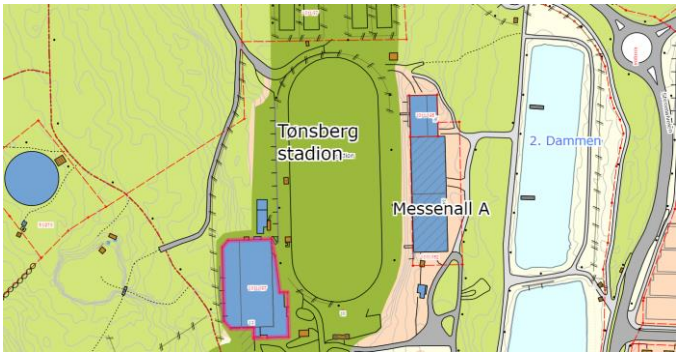

Figure 4: Map of the area, Tønsberg municipality website

C. *Site roughness evaluation*

The wind of the area should be modelled, in order to accurately simulate the wind effects on the arena. As previously mentioned, the roughness and terrain of the area around the Maier arena slows the wind down uniquely to that area, and thus produces a velocity profile. Therefore, a site analysis is needed. An overview picture of the area, obtained from google earth, is helpful in order to determine the terrain roughness category.

Figure 5: Maier arena aerial photo, google earth.

From Fig. 5 the following can be observed. Directly south of the arena there are buildings. To the north northeast, there are buildings and forest. To the east and west, first forest, then farmlands. When choosing roughness factor, worst case roughness factors should be used [6]. When modelling the atmospheric velocity profile, the α value for cultivated land with scattered buildings is chosen. The factor is found to be 0.16, by the recommended practices by DNV, table 2-1 [3].

D. Tønsberg meteorological data

Meteorological data is of interest in order to determine the main direction and magnitude of the wind. From the Norwegian meteorological institutes website [7], the wind roses for short and long term from the nearest meteorological measuring station was obtained. Presented Fig. 6-7. The Melsom station is 8 km to the south, and slightly to the west of the arena building site.

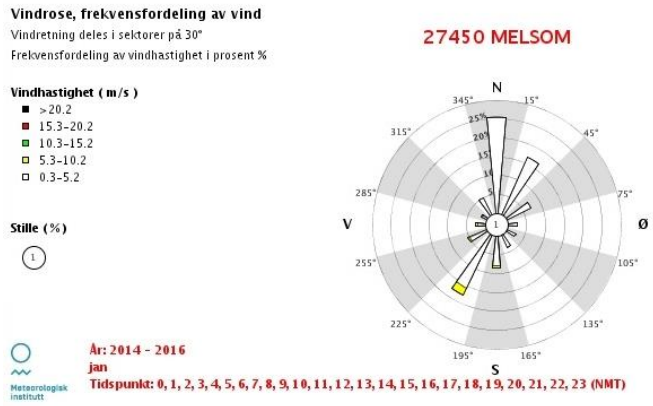

Figure 6: Melsom wind rose, frequency distribution of wind, 2014-2016, meteorological institute

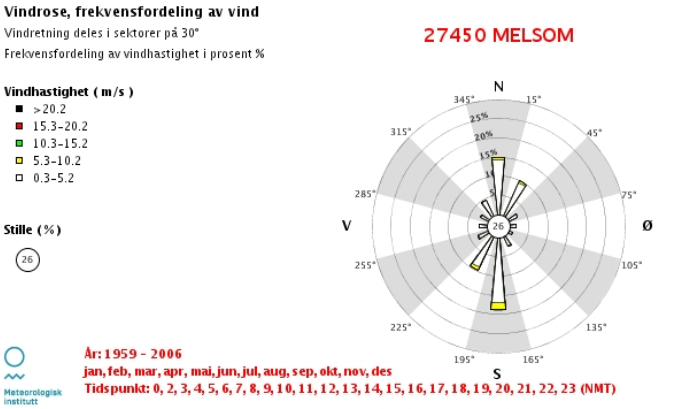

Figure 7: Melsom wind rose, frequency distribution of wind, 1959-2006, meteorological institute

See Fig. 6-7, one can observe that the dominating high speed wind direction is from south, southwest. Some wind from north is also to be expected. Wind speed of this area rarely exceeds 5.2 m/s, and even rarer 10.2 m/s.

E. Wind tunnel testing

Wind tunnel testing of small scale models can be a cost effective way to determine wind effects. The validity of wind tunnel testing will be investigated and discussed in the literature review. The wind tunnel at the department of energy and process engineering at NTNU was used in this project. The test section is two meters tall and three meters wide and has a max speed of 27 m/s [8].

F. Atmospheric velocity profile

In order to model the atmospheric velocity profile, roughness elements were inserted. The elements covered homogeneously the entire width of the test section, and had a distribution length in the flow direction of 1.2 m. The roughness elements were positioned at the inlet of the wind tunnel test section. See Fig. 8.

Figure 8: Roughness elements

The velocity profiles were measured using a pitot tube mounted on a traverse. See Fig. 9. The traverse is capable of moving in width x and height z. The

velocity profiles were measured at five positions. In the middle of the wind tunnel i.e. x equal 0 mm, plus minus 300 mm and plus minus 670 mm. The velocity profiles were measured at two different wind speeds, 2.5 m downstream from the roughness elements. Measurements started at the ground, z equal to 0, and increased 1.5 mm for each measurement.

Differential pressure transducer signals were amplified and routed to a data acquisition unit connected to a computer. When measuring the dynamic pressure, positive pressure was stagnation pressure, negative was static pressure. A second pressure transducer measured the pressure difference before and after the contraction chamber in the wind tunnel. This pressure can be related to the inlet wind speed by continuity and assuming incompressibility. Temperature and atmospheric pressures were also recorded for each experiment. The voltage was measured with 15000 samples at a frequency of 1000.

Figure 9: Pitot tube mounted on the traverse

The nondimensionalized velocity profiles, are shown in Fig. 10, together with a dimensionless power law velocity profile. It was obtained using an α of 0.16, scaled down reference height of 66 mm, and a wind speed at reference height equal to 7.2 m/s. The velocity profiles measured in the wind tunnel were nondimensionalized by dividing by the freestream velocity i.e. at z equal to 500 mm. The power law velocity profile was nondimensionalized by dividing by 10 m/s, which is the wind speed of the velocity profile at z equal to 500 mm.

From Fig. 10 one can observe an increase in wind speed off-center in the wind tunnel. The dimensionless velocity profiles for two different wind speeds are nearly identical. The velocity profile generated by the roughness elements is therefore determined to be Reynolds number independent. In addition, the velocity profiles at plus minus 300 mm and 670 mm, respectively, are closely aligned. It is therefore reasonable to assume that the velocity profiles, in the width direction of the wind tunnel are symmetrical about the middle. The generated velocity profile is not uniform across the width. This is likely caused by the large disc which the model arena is positioned on. The disc is 2.4 m in diameter, positioned in the middle of the test section, which means it does not affect the entire test section, higher wind speeds at the walls is to be expected.

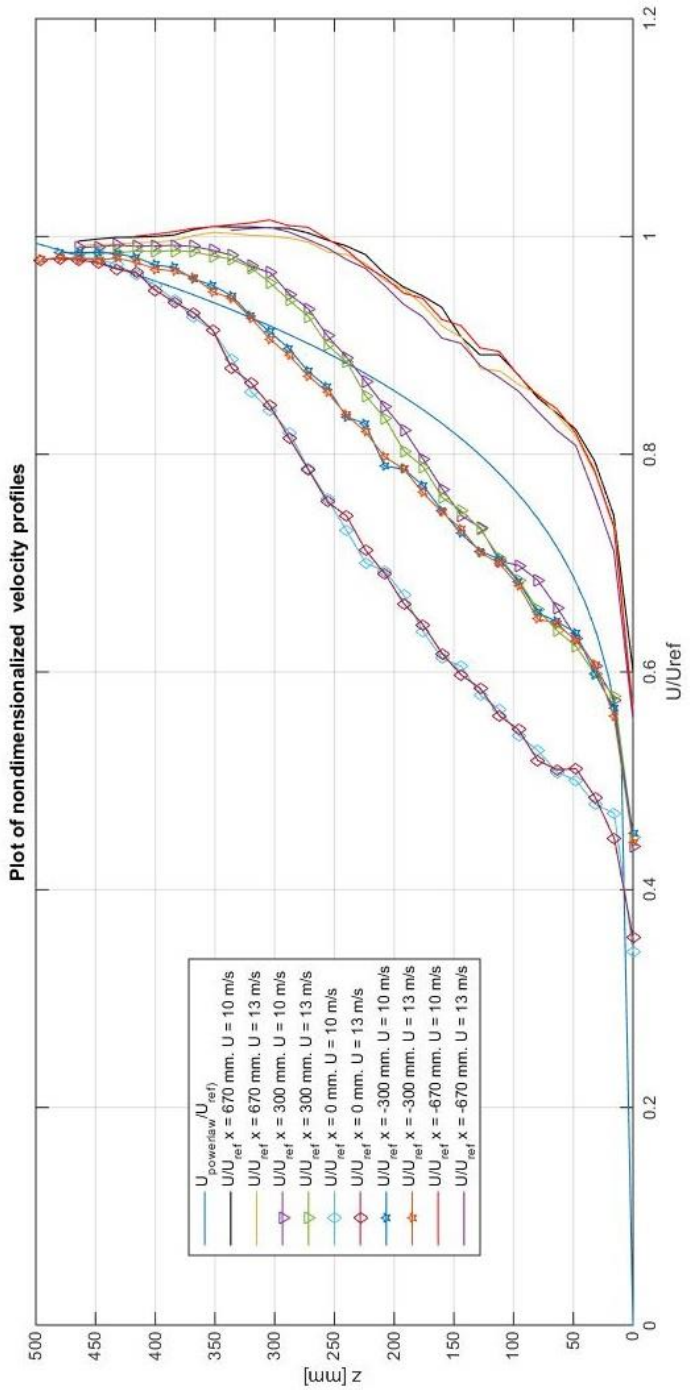

Figure 10: Plot of dimensionless velocity profiles

IV. Wind tunnel testing

A. Types of wind tunnel experiments

1) Measuring the mean pressure difference at the four sections of the model arena, relative to the free stream during wind speeds equal to 9.6 m/s and 12.8 m/s. Logged using the same equipment and settings as during velocity profile measurements.

2) Flow visualization of direction, at wind speed equal to 6 m/s. Achieved by using tufts and photographing. Goal was to visualize areas of flow recirculation.

3) Flow visualization of powder distribution. Wind speed of 6 m/s and 11.5 m/s. Photographing the results. goal was to visualize the areas where separation, reattachment and recirculation occurs, and where it does not.

B. Wind tunnel experiments setup

The wind tunnel has a close to uniform and nearly laminar flow. As mentioned previously, the velocity profiles were nondimensionalized by dividing by the free stream velocity. The same was done for the mean pressure experiment.

Atmospheric pressure varies day by day. The temperature of the air in the wind tunnel also varies. Ambient temperature also varies, however, fluctuation in air temperature is mainly caused by the heat generated by friction. The friction is caused by the rotating machinery. Air density changes due to variations in temperature and atmospheric pressure. To enable corrections, these parameters were also recorded. However, when nondimensionalizing the velocities, the density term cancels out and is insignificant.

The roughness elements used to model the velocity profile in shown in Fig. 8 was present during all experiments. All three experiment types were carried out at three angles of attack, south, southwest, west, with and without the bricks representing the nearby structures. See Fig. 11-12.

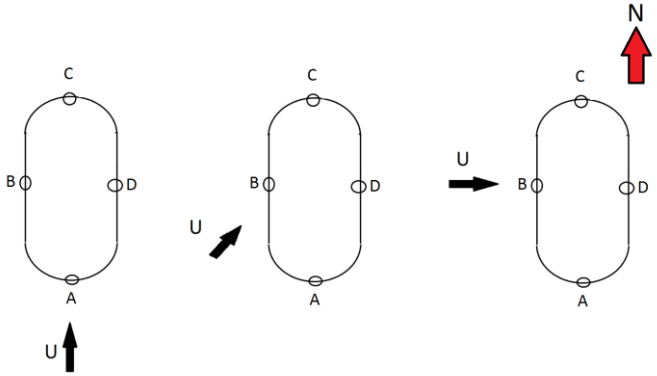

Figure 11: Sketch showing wind directions and pressure tap sections

Figure 12: Experiment setup, with bricks representing nearby structures

V. Results

A. Mean pressure coefficient distribution

The mean pressure coefficients measured at the different wind speeds were practically the same, with less than 0.01 difference. Except one point. It will be noted and discussed before presenting the data. At the pressure tap closest to ground, section D, with wind from south and with nearby structures (Fig. 14), the experiment at 12.8 m/s produced a positive pressure coefficient of 0.06. compared to the suction of 0.02 found at 9.6 m/s. Considering that the equivalent experiment without buildings (Fig. 13) found suction of 0.01 at both wind speeds, this could indicate that at this wind speed the nearby structure generates small-scale-turbulence which controls the pressure [9]. This is also in agreement with the findings of [10], which states; “while high pressures or suctions are often reduced in complex surroundings, the lower loads increase. This reduction of mean loads and increase of dynamic loads due to increased turbulence in the cluttered environment result in an increase of the lower peak loads”. These changes occur because surrounding buildings increase turbulence and redirects the wind.

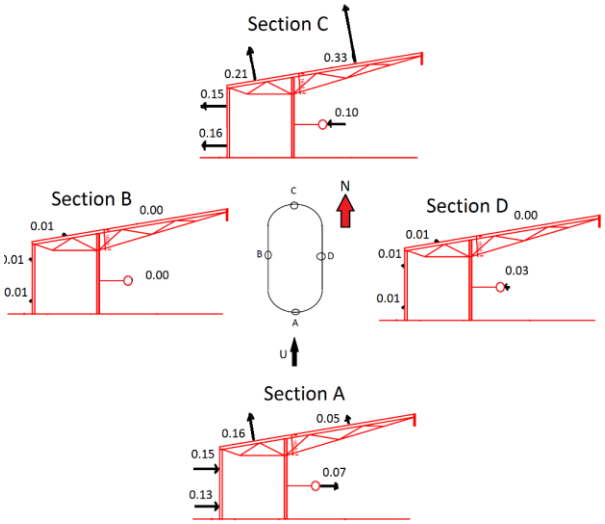

Figure 13: Pressure distribution, south, open land

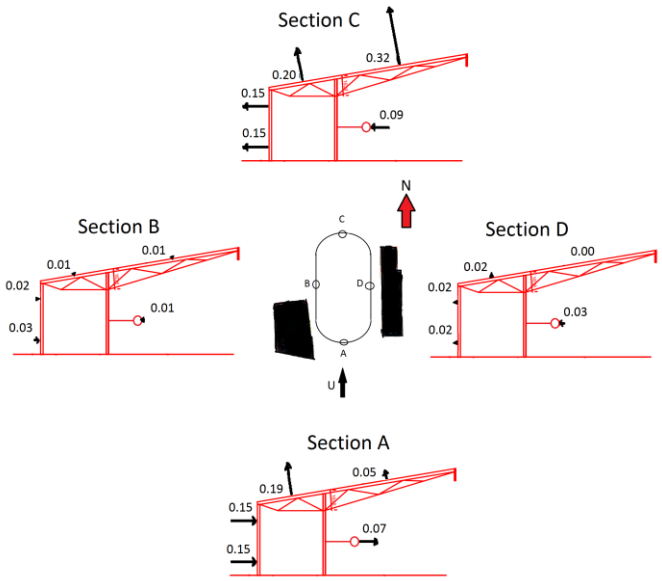

Figure 14: Pressure distribution, south, nearby structures

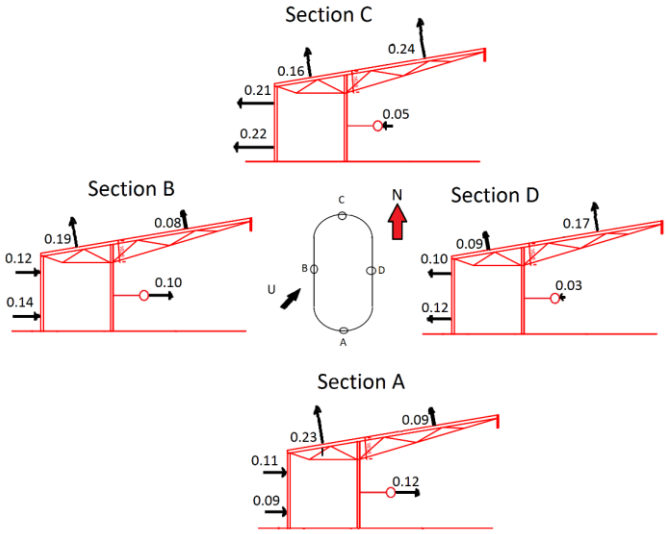

Figure 15: Pressure distribution, southwest, open land

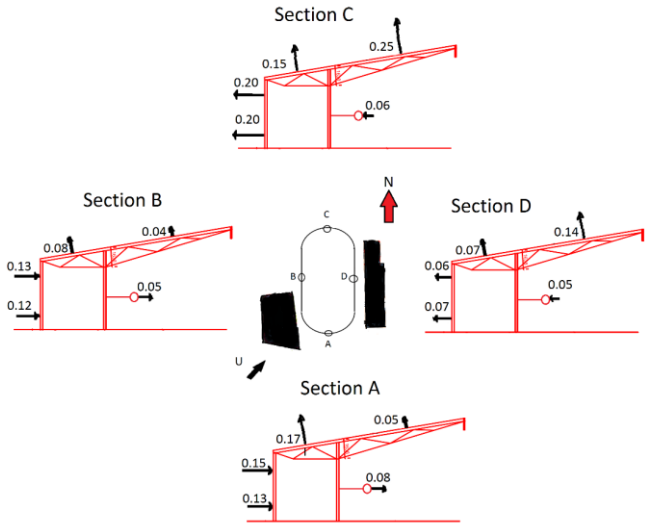

Figure 16: Pressure distribution, southwest, nearby structures

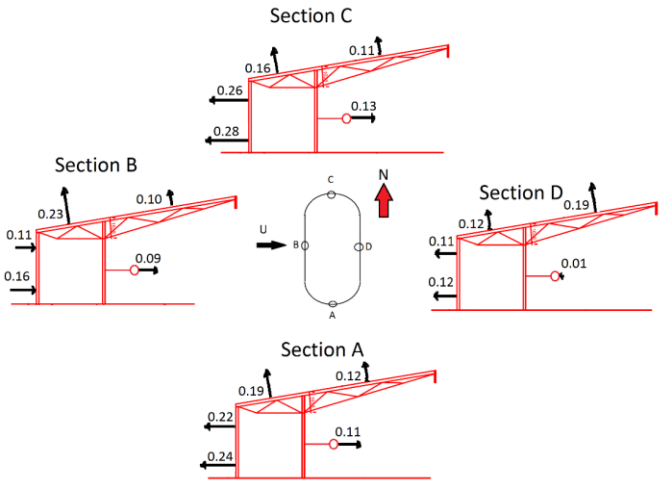

Figure 17: Pressure distribution, west, open land

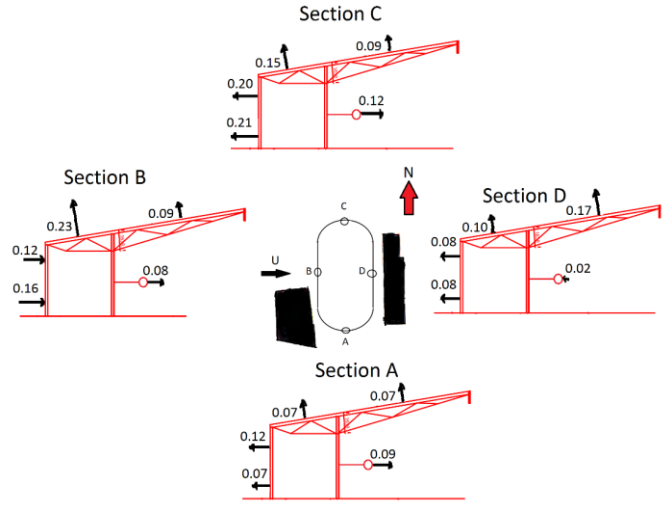

Figure 18: Pressure distribution, west, nearby structures

B. *Flow visualization: Direction*

Figure 19: South, open land, overview

Figure 20: South, nearby structures, overview

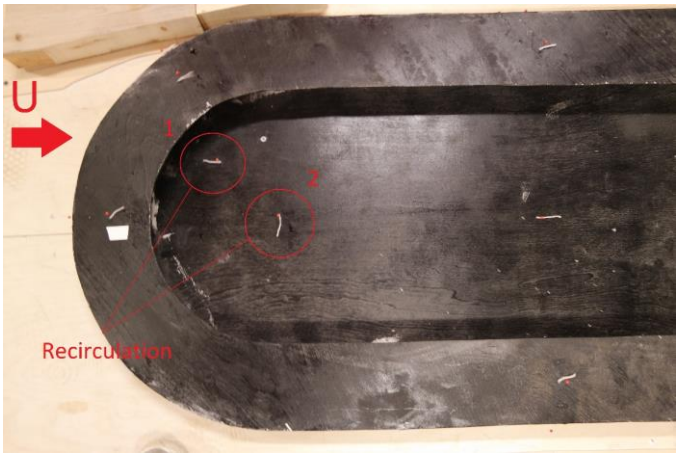

Figure 21: South, nearby structures, close-up

Figure 22:Southwest, open land

Figure 23: Southwest, open land. Note the horizontal tuft

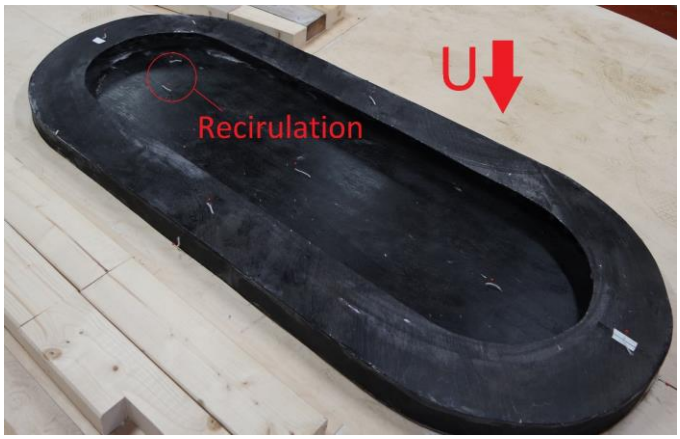

Figure 24: Southwest, nearby structures, overview

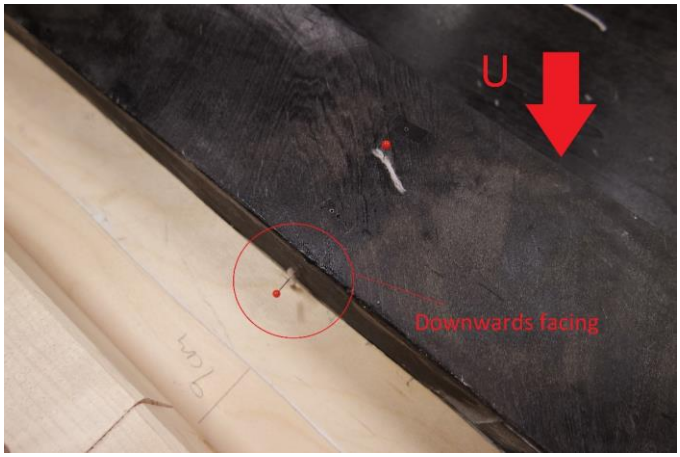

Figure 25: South west, nearby structure.

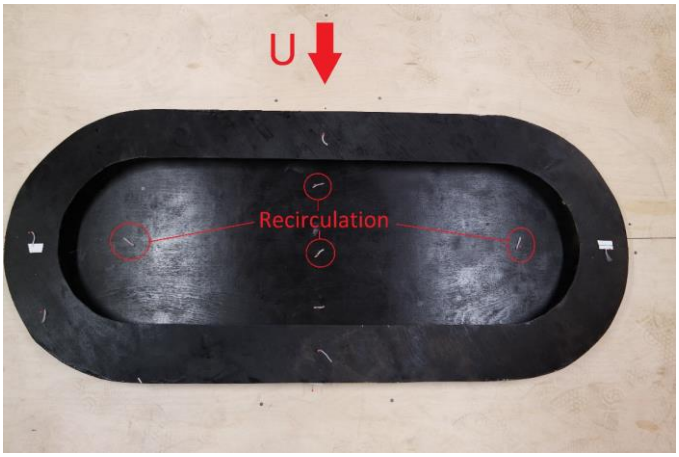

Figure 26: West, open land

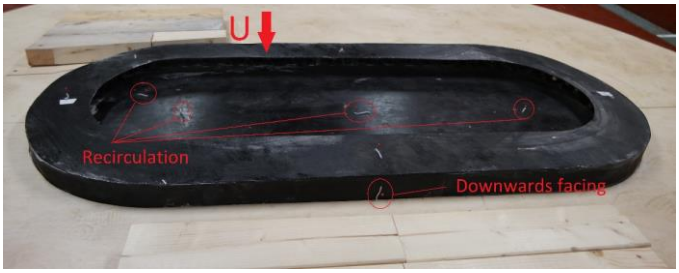

Figure 27: West, Nearby structures overview

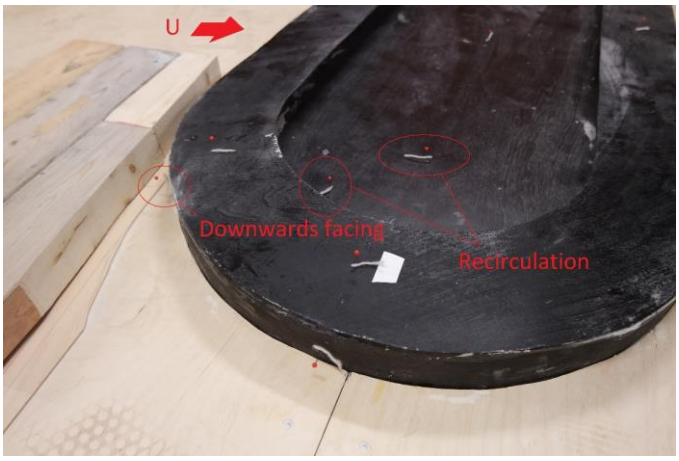

Figure 28: West, nearby structures close-up

C. *Flow visualization: Powder*

Figure 29: Initial evenly distributed powder

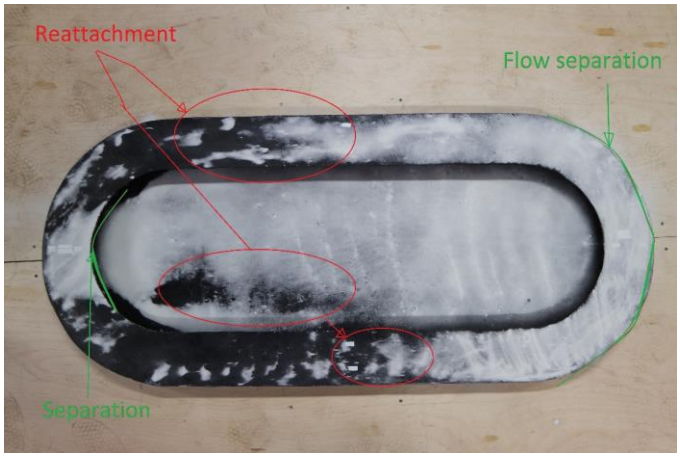

Figure 30: South, open land, 6 m/s

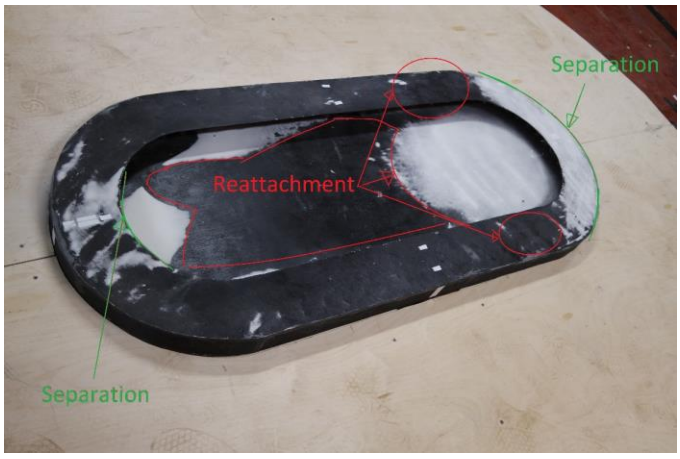

Figure 31:South, open land, 11.5 m/s

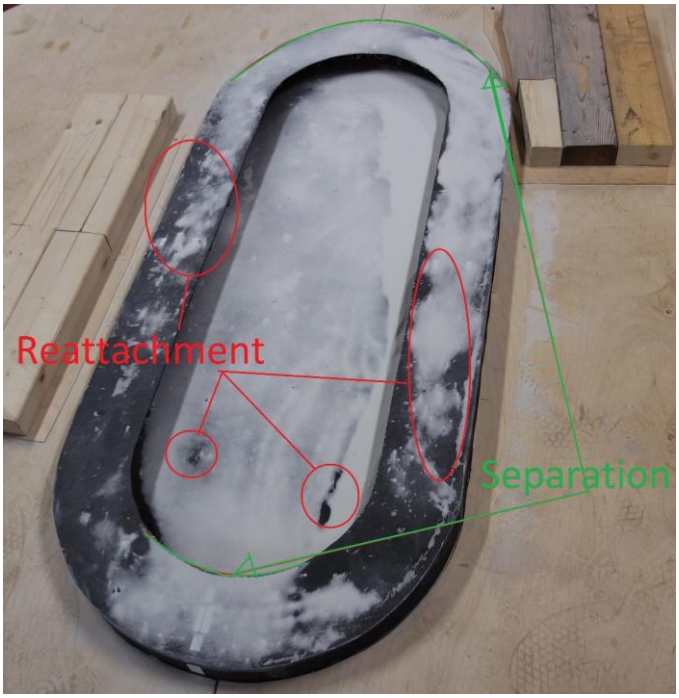

Figure 32: South, nearby structures, 6 m/s

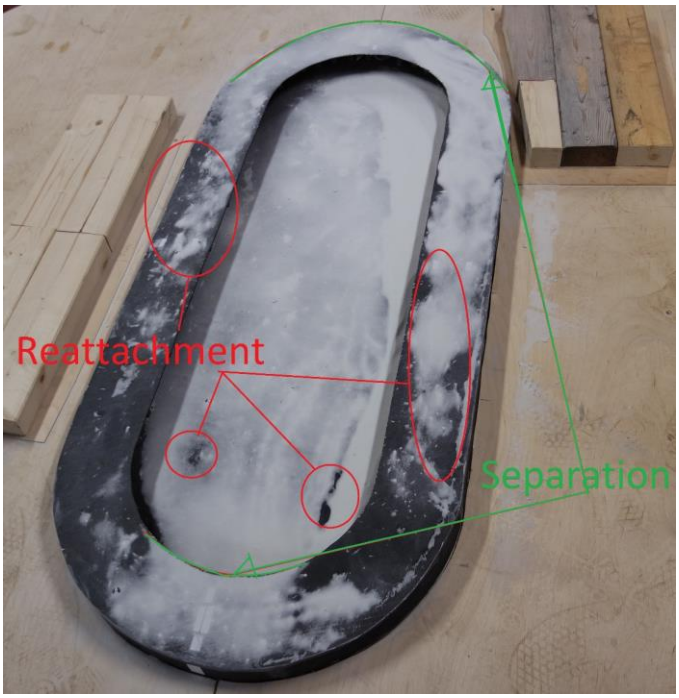

Figure 33: South, nearby structures, 11.5 m/s

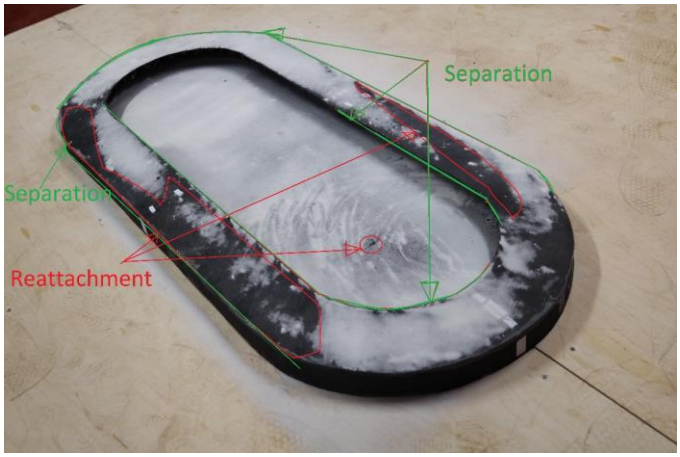

Figure 34: Southwest, open land, 6 m/s

Figure 35: Southwest, open land, 11.5 m/s

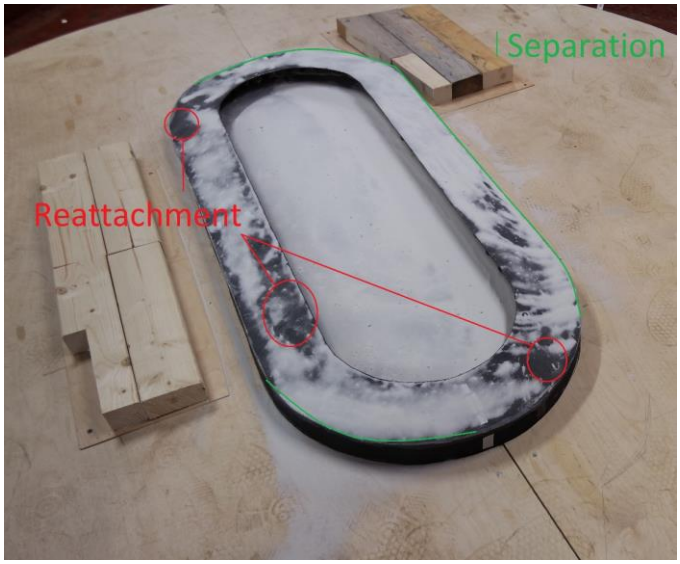

Figure 36: Southwest, nearby structures, 6 m/s

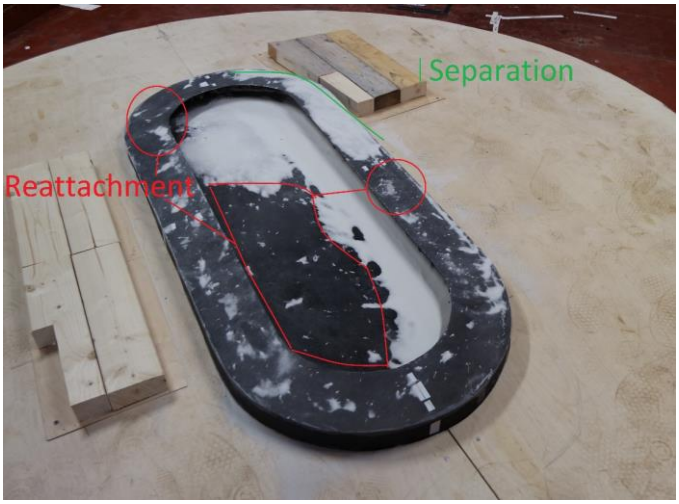

Figure 37: Southwest, nearby structures, 11.5 m/s

Figure 38: West, open land, initial powder distribution. Note the powder was spread using fingers, hence the pattern

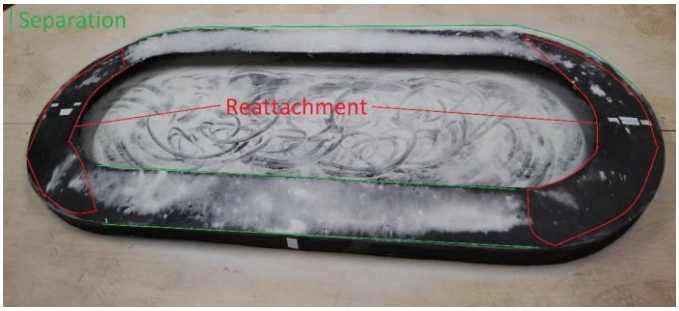

Figure 39: West, open land, 6 m/s

Figure 40: West, open land, 11.5 m/s

Figure 41: West, nearby structures, 6 m/s

Figure 42: West, nearby structures, 11.5 m/s

VI. Discussion

A. Mean pressure coefficient distribution

The difference between all the pressure coefficients obtained at two different wind speeds were, with the exception of one point, less than 0.01. This indicates that the results are Reynolds number independent.

1) South, with and without nearby structures

Fig. 13, section A, increasing positive pressure coefficients in the vertical direction at the wall were observed. Positive wall pressure is caused by the flow meeting the wall, leading to reduction in wind speed. The result was 0.13 at ground, and 0.15 farther up. This increase in pressure vertically at walls is in good agreement with previous findings [11]. For Fig. 14 however, the wall pressure coefficients stayed constant, at 0.15.

For both experiments, section A, on the roof and under the roof, suction was observed. The suction is caused by the wind speed increase due to the sudden change in geometry. Fig. 13, roof section A, the windward edge's tap produced a suction about three times higher, 0.16, compared to the second tap, 0.05. Fig. 14, roof section A, about four times higher suction at the windward edge tap, 0.19, was observed. For both experiments, a suction of 0.07 was observed under the roof.

Section B and D produced no significant values during either open land or nearby structures experiments, highest being wall and under roof pressure of 0.03. This indicates the wind on the roof has reattached.

Finally, section C for Fig. 13-14 produced the highest roof suction of all, on the windward edge tap, 0.33, the second, 0.21. When adding structures, the roof suction on section C changed max 0.01, i.e. no significant change. The flow has once again been forced to separate. Observed higher degree of suction produced when the flow meets the tall side of the roof at the north end. Under the roof, positive pressure of 0.10 The pressure taps on the wall of section C produce suction as well, about 0.15.

2) Southwest with and without nearby structures.

These experiments, did not provide higher roof suction than the ones previously discussed. Higher wall suction was observed, however.

See Fig. 12 for southwest wind, section A is not directly behind the wake of the structure. Nevertheless, the pressure experiments (Fig. 15-16) clearly show a degree of influence by the structure on section A. The structure is providing cover and reducing roof suction. The wall pressures are increasing. This is likely due to the same phenomena discussed previously before presenting the results, the structure redirects the wind and increase turbulence. The added structures reduce suction on the roof of section A.

At Section B, the inclusion of the structure more than halves the roof suction. The wall pressures are quite unaffected. Section C is more or less unaffected by the inclusion of structures. Section D experienced a slight reduction of both wall and roof suction.

3) West, with and without nearby structures

See Fig. 12, west wind, section A is clearly located directly behind the added structure. A reduction of both wall and roof suction is observed.

When adding structures, section B is rather unaffected, whereas section C and D experience some reductions of wall suction due to the added structures.

The results obtained at section B does not directly mirror the results at section A for wind from south. The walls are not curved here, and the width is increased, leading to the wind behaving differently. In fact, at the wall, a higher pressure close to ground, 0.16, is observed, compared to farther up, 0.11. With wind from west, the roof experiences higher suction on section B, compared to what was measured with wind from south on section A.

Narrow buildings of half the width, have previously been shown to produce, on average, both mean and peak roof pressure coefficients approximately 20% higher [12]. This was not the case when looking at the results from section A with wind from south compared to section B with wind from west. The roof suction is not increased in the experiment with wind from south at section A. This could be because the wall is not just narrowed, it is also curved, leading to less sharp geometry changes, leading to less flow disturbance, and this possibly being the reason for the lower wall pressure at the ground, and likely the reason for the lowered roof suction.

The highest measured wall suction was measured on Fig. 17, section C, wall suction equal to 0.28. This was the maximum wall suction of all experiments. When adding structures (Fig. 18), the suction was reduced, even though the structures are clearly not upstream of the section. The structures probably affect section C by slowing the wind speed in general around the model.

Table 1:

Dimensioning Pressure coefficients, open land		
Wall Pressure	Wall Suction	Roof Suction
0.16	0.28	0.33

Table 2:

Dimensioning Pressure coefficients, nearby structures		
Wall Pressure	Wall Suction	Roof Suction
0.16	0.21	0.32

B. Flow direction visualization

It has previously been performed flow visualization on the roof of the Texas Tech building [13], by using tufts. Investigation of the flow directions, at the Maier arena model, has been performed by using tufts. The tufts facing inwards towards the arena, the opposite direction of the flow, indicate flow separation and recirculation under the roof of the Maier arena. See Fig. 21, tuft #1 points inwards. Tuft #2 points towards east. At these points, the tufts indicate flow circulation. The same inwards facing tufts can be observed for southwest and west. See the marked tufts Fig. 24 and Fig. 26.

Southwest, with structures (Fig. 25) compared to the equivalent with open land (Fig. 23) one can observe that wind speed around the arena is reduced by the surrounding buildings. With wind from west with structures (Fig. 28) there is also lowered wind speed as indicated by the downwards facing tuft. For these wind directions the surrounding buildings add some shelter.

C. Flow visualization using powder

From the powder distribution for the different wind speeds and wind directions, with and without nearby structures, some general trends can be observed. See Fig. 30-42, the areas of interest, mainly separation and reattachment have been identified.

All experiments show a degree of cover under the roof. In addition, one can observe a lack of powder removal on the roof at the leading edges. This is caused by the separation occurring when the wind meets the model's edge, leading to increased wind speeds, lowered pressure and detached boundary layer. It is the sudden change in geometry with a decrease in available area for the wind, which leads to the increased wind speed and detachment over roof. Downstream, the flow reconnects to the roof and ground. Powder is removed and suction is lowered on roof, as observed by the pressure experiment. Wind from southwest (and southeast, northwest, northeast due to symmetry) lead to highest degree of powder accumulation on roof and ground.

In general, the addition of buildings produces additional areas of cover and less overall powder removal. This indicates that the surrounding

buildings will separate and deflect the flow. The overall result is that the wind will slow down.

VII. Literature Review

A. Validity of wind tunnel testing of scale models

Wind tunnel testing of small scale models is a method to determine the wind effects on buildings. However, full scale validation is preferable. In the past there has been found reasonable agreement between model-scale and full-scale results [14]. In particular, the agreement between full scale and small scale mean wind-pressure coefficients has been found to be good [15]. Also, wind tunnel testing has been found to be a good way to verify the results obtained from computational fluid dynamics [16].

One of the challenges in obtaining the same results when validating full-scale experiments, is the inability to control for the vast variety of geometry upstream [17]. Wind tunnels produce a wind that is much easier to control.

B. Mono sloped roof research

The Maier sports arena has a mono-sloped roof with no corners. According to [13], experimental data indicate that both mean and instantaneous peak wind pressures are higher on mono-sloped roof than gabled roofs. In addition, the authors found that the suction is highest on the windward edge of the roof, and decreasing with increasing distance onto the roof. This trend held true for all wind directions. The same results have been obtained for the model Maier arena. Further it was found that at a wind direction of 45 degrees onto a sharp corner, the highest suction was observed [13]. As mentioned before, the Maier arena has no sharp corners, so this leads to lower peak values. The researchers also found that how close the pressure tap was to the windward edge, played a significant role in how much suction was observed. When wind direction was directly onto the lower height side of the roof, max suction (-1.0) was found to be 5 times larger than the lowest suction (-0.2). The test building had a roof with an incline of 6°. Similar to the Maier arena's 5.8°.

The same paper further states that roof suction is mostly affected by height, whereas wall pressures are rather insensitive to the building height.

C. Maximum loads

The maximum loads affecting buildings are of interest when dimensioning the structure. For many insurance cases it has been found that failure of roofs near corners, edges and ridges was the reason for failure and the main reason for wind damage occurring [10]. Maximum loads occur for peak wind, not mean wind. Appropriate safety margins when accounting for wind gusts should therefore be considered as well.

D. Human Wind comfort

In order to determine the human wind comfort, one must evaluate the maximum acceptable wind speed. Koss [17] made a thorough comparison of wind comfort criteria, and presented an overview of comfort criteria available. Koss found there to be good agreement between the published criteria, meaning most comfort criteria can safely be utilized. According to the NEN8100, 5.0-10 m/s is acceptable for strolling and traversing, but not sitting [18]. This is the maximum wind speeds obtained from the meteorological data. This indicates that the spectators, due to cover of the roof will at most cases be at comfortable wind speeds. The athletes on the ice might experience some wind effects, as demonstrated by the reattachment of the wind. However, ice skating performance should be unaffected most of the time.

VIII. Conclusion

The maximum values for the mean pressure coefficients were: Maximum wall pressure, 0.16. Maximum wall suction, 0.28. Maximum roof suction, 0.33. The lack of sharp corners on the Maier arena will make the worst cases less severe. However, the mean wind pressure coefficients obtained do not take into account gust wind speeds. Appropriate safety factors should be applied when dimensioning.

The visualization experiments have successfully shed light onto the wind behavior and effects on the arena. The areas of recirculation, separation and reattachment have been identified for several wind directions. The areas of recirculation indicate some wind effects toward the spectators. The reattachment onto the ground indicate that the athletes will be affected by wind, but according to most standards, the wind is tolerable for strolling and traversing. The worst case for accumulation of

powder was found to be be wind from a 45-degree angle (southwest, southeast, northwest, northeast).

In addition, the downwards facing tufts indicate that low wind speeds and shelter will be present at certain points around the arena. The meteorological data also indicates acceptable wind speeds according to comfort criteria.

A concluding remark; the experiments and results obtained should be validated by further research. The scaled down model arena was built by hand and is not a 100% accurate representation of the real arena. Some errors when building occurred, particularly in the height of the roof. The scale is actually 1:132 in height. Previous research has shown that the wall pressure is rather insensitive to height, whereas the roof pressure is. CFD validation of an accurate 3D model would be of interest, and when the full scale arena is built, a full scale validation could be undertaken.

REFERENCES

[1] Day, M.A. (1990). "The no slip-condition of fluid dynamics". Erkenntnis vol. 33 no. 3, November, pp. 285-296.

[2] Dalgliesh W.A. and D.W. Boyd (1962). "Wind on Buildings". Canadian Building Digest vol. 28. April

[3] DNV (2007) "Recommended Practice DNV-RP-C205 Environmental Conditions and Environmental Loads". April.

[4] Cengel, Y.A and Cimbala J.M (2006). "Fluid mechanics: fundamentals and applications", 1st ed. New York: McGraw-Hill

[5] Abbot, I.H. and Von Doenhoff, A.E (1959) "Theory of Wind Sections". New York: Dover Publications, Inc.

[6] Noreng K. and Strandholmen B. (2004). "Vindlast på flate tak. Innfesting av fleksible takbelegg". Byggforsk, Norges byggforskningsinstitutt

[7] (2016). www.met.no

[8] (2016). https://www.ntnu.edu/ept/laboratories/aerodynamic

[9] Tieleman, H.W. Surry, D. and Mehta, K.C. (1996) "Full/model-scale comparison of surface pressures on the Texas Tech Experimental building". Journal of Wind Engineering and Industrial Aerodynamics vol. 61, pp 1-23

[10]Ho, T.C.E. Surry, D. and Davenport A.G. (1991). "Variability of low building wind loads due to surroundings". Journal of Wind Engineering and Industrial Aerodynamics vol. 38, pp 297-310.

[11]Olsson, H.A. (1974). "Vindtryck inuti byggnader". Stockholm: Tekniska högskolan i stockholm, Institutionen för konstruktionslära.

[12] Stathopoulos, T. and Mohammadian, A.R. (1986). "Wind loads on low buildings with mono-sloped roofs". Journal of Wind Engineering and Industrial Aerodynamics vol. 23, pp 81-97.

[13]Sarkar, P.P. Zhao, Z. Mehta, K.C. (1997). "Flow visualization and measurement on the roof of the Texas Tech Building". Journal of Wind Engineering and Industrial Aerodynamics vol. 69-71, pp 597-606.

[14]Surry, D. (1991). "Pressure measurements on the Texas Tech Building: Wind tunnel measurements and comparisons with full scale". Journal of Wind Engineering and Industrial Aerodynamics vol. 38, pp 235-247.

[15]Okada, H. and Ha, Y. (1992) "Comparison of Wind Tunnel and Full-Scale Pressure Measurement Tests on the Texas Tech Building". Journal of Wind Engineering and Industrial Aerodynamics vol. 41-44, pp 1601-1612.

[16]Santiago, J.L. Martilli, A. and Martín, F. (2007). "CFD simulation of airflow over a regular array of cubes. Part I: Three-dimensional simulation of the flow and validation with wind-tunnel measurements". Boundary-Layer Meteorol vol. 122, pp 609-634.

[17]Koss, H.H. (2006). "On differences and similarities of applied wind comfort criteria". Journal of Wind Engineering and Industrial Aerodynamics vol. 94, pp 781-797.

[18]Blocken, B. and Persoon, J. (2009). "Pedestrian wind comfort around a large football stadium in an urban environment: CFD simulation, validation and application of the new Dutch wind nuisance standard". Journal of Wind Engineering and Industrial Aerodynamics vol. 97, pp 255-270